

AD-A261 197



2



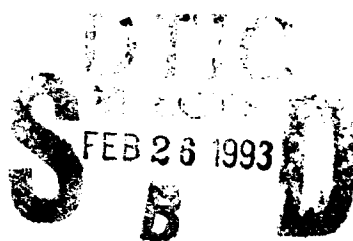
Research and Development Technical Report
SLCET-TR-91-18

Use of Permanent Magnets in Magnetron Design

Anup S. Tilak, Herbert A. Leupold and
Ernest Potenziani II

Electronics Technology and Devices Laboratory

July 1991



DISTRIBUTION STATEMENT
Approved for public release.
Distribution is unlimited.

715129



93-04082

U. S. ARMY LABORATORY COMMAND
Electronics Technology and Devices Laboratory
Fort Monmouth, NJ 07703-5601

NOTICES

Disclaimers

The findings in this report are not to be construed as an official Department of the Army position, unless so designated by other authorized documents.

The citation of trade names and names of manufacturers in this report is not to be construed as official Government indorsement or approval of commercial products or services referenced herein.

REPORT DOCUMENTATION PAGE

Form Approved
OMB No. 0704-0188

Public reporting burden for this collection of information is estimated to average 1 hour per response, including the time for reviewing instructions, searching existing data sources, gathering and maintaining the data needed, and completing and reviewing the collection of information. Send comments regarding this burden estimate or any other aspect of this collection of information, including suggestions for reducing this burden, to Washington Headquarters Services, Directorate for Information Operations and Reports, 1215 Jefferson Davis Highway, Suite 1204, Arlington, VA 22202-4302, and to the Office of Management and Budget, Paperwork Reduction Project (0704-0188), Washington, DC 20503.

1. AGENCY USE ONLY (Leave blank)		2. REPORT DATE July 1991	3. REPORT TYPE AND DATES COVERED Technical Report: 1990-1991	
4. TITLE AND SUBTITLE USE OF PERMANENT MAGNETS IN MAGNETRON DESIGN			5. FUNDING NUMBERS PE: 060110 PR: 1L161102AH47 TA: 01 WU: 04 DA302913	
6. AUTHOR(S) Anup S. Tilak, Herbert A. Leupold and Ernest Potenziani II				
7. PERFORMING ORGANIZATION NAME(S) AND ADDRESS(ES) US Army Laboratory Command (LABCOM) Electronics Technology and Devices Laboratory (ETDL) ATTN: SLCET-EA Fort Monmouth, NJ 07703-5601			8. PERFORMING ORGANIZATION REPORT NUMBER SLCET-TR-91-18	
9. SPONSORING / MONITORING AGENCY NAME(S) AND ADDRESS(ES)			10. SPONSORING / MONITORING AGENCY REPORT NUMBER	
11. SUPPLEMENTARY NOTES				
12a. DISTRIBUTION / AVAILABILITY STATEMENT Approved for public release; distribution is unlimited.			12b. DISTRIBUTION CODE	
13. ABSTRACT (Maximum 200 words) Several alternative designs for a magnetron/gyrotron, permanent-magnet solenoid are analyzed with regard to magnetic field uniformity and magnitude, structural weight, susceptibility to heating, and access hole size. Structural masses were found to range from about 10 kilograms to 60 kilograms depending on details of design and or the type of permanent magnet tube. Recommendations are made as to the best choices for the intended purpose.				
14. SUBJECT TERMS Permanent-magnet solenoids; magnetrons; gyrotrons; magnetic cladding; azimuthal dependence of field			15. NUMBER OF PAGES 30	
			16. PRICE CODE	
17. SECURITY CLASSIFICATION OF REPORT Unclassified	18. SECURITY CLASSIFICATION OF THIS PAGE Unclassified	19. SECURITY CLASSIFICATION OF ABSTRACT Unclassified	20. LIMITATION OF ABSTRACT UL	

Table of Contents

<u>Section</u>	<u>Page</u>
Introduction.....	1
Design Specifications.....	1
Theory.....	1
Preliminary Investigation: Possible Configurations.....	6
A. Ideal Case.....	6
B. Worst Case.....	6
C. Intermediate Case.....	10
Effect of Waveguide Ports on Field Uniformity.....	10
Final Analysis.....	13
Conclusions.....	14
References.....	16
Appendix A • Three-Dimensional Analysis.....	17

Accession For	
NTIS GPO&I	<input checked="" type="checkbox"/>
DTIC TAB	<input type="checkbox"/>
Unannounced	<input type="checkbox"/>
Justification	
By _____	
Distribution/	
Availability Codes	
Dist	Availability
A-1	

List of Figures

<u>Figure</u>	<u>Page</u>
1. Longitudinal cross section of magnetron	2
2. Transverse cross section of magnetron	3
3. (a). Determination of supply magnet cross-section. (b).Determination of cladding thickness	4
4. Design for a traditional symmetrically cladded constant field permanent magnet solenoid	5
5. Three alternatives for permanent magnet placement in a magnetron	7
6. A 2-D finite element plot for the ideal case design	8
7. Field profile in the interaction region of the ideal design	8
8. A 2-D finite element plot for the worst case design	9
9. Field profile in the interaction region of the worst case design	9
10. Magnet location in the intermediate choice	11
11. Magnet mass and magnetic field summary for the three choices	12
12. A 2-D finite element plot for the most practical design	13
13. Field profile in the interaction region of the best choice	14
14. Permanent magnet choices for magnetrons; a summary	15
15. Variation in peak field as a function of tunnel radius	16
A-1. Side view of the overall structure as used in the three-dimensional analysis	18
A-2. View of cut through section A of Figure A-1	19
A-3. Diagram of a cut through section B of Figure A-1	19
A-4. Diagram of a cut through section C of Figure A-1	20
A-5. Diagram of a cut through section D of Figure A-1	20
A-6. Overall view of the various solids making up the structure ($1/2$ length and 180° of revolution)	21
A-7. Resulting three dimensional finite element mesh of the structure of Figure A-6	22
A-8. H_z versus distance along z-axis, $\theta = 45^\circ$	23
A-9. H_z versus distance along arc from $\theta = 0^\circ$ to $\theta = 180^\circ$ at $r = 2.1$ cm	23
A-10. H_z versus distance along arc from $\theta = 0^\circ$ to $\theta = 180^\circ$ at $r = 4.5$ cm	24

USE OF PERMANENT MAGNETS IN MAGNETRON DESIGN

INTRODUCTION

All magnetrons require a cathode and an anode with a dc magnetic field perpendicular to the dc electric field between them. The electrons emitted by the cathode are influenced by the crossfields to move in curved paths in the interaction region. They continue to drift towards the positively polarized anode where they are ultimately collected.

This study deals with the feasibility of permanent magnet field sources in magnetrons. A dc magnetic field of about 7.5 kOe $\pm 5\%$ was required in an interaction region that is 7.2 cm long and 0.53 cm wide. Several suitable options were investigated and are compared in this report.

DESIGN SPECIFICATIONS

Figure 1 shows the longitudinal cross section of the magnetron that was the subject of this investigation and Figure 2 shows its transverse cross section. As indicated in Figure 2, the outer radius of the cathode R_1 is 1.58 cm and the inner radius of the anode, R_2 , is 2.11 cm. The interaction region, between the anode and the cathode, is 0.53 cm across; and the outer radius of the anode block, R_4 , is 4.62 cm. The cavity angles in the anode block are 20° and two of the cavities, diametrically across from one another, serve as entry ports for the waveguides needed for the rf output. The waveguide extends 7.0 cm along the 7.2 cm length of the structure. The dc electric field and the magnetic field are respectively perpendicular and parallel to the structural axis.

THEORY

Details of a clad cylindrical longitudinal field structure have been described elsewhere.¹⁻³ Provisions for a field $H_W = 7.5$ kOe in a cylindrical space of radius 4.62 cm and length 7.20 cm requires a flux Φ_W in the interaction region of

$$\Phi_W = \pi R_4^2 H_W = 503 \text{ kMx} \quad (1)$$

This flux is to be supplied by a longitudinally oriented magnet encompassing the working space as shown in Figure 3. Hence,

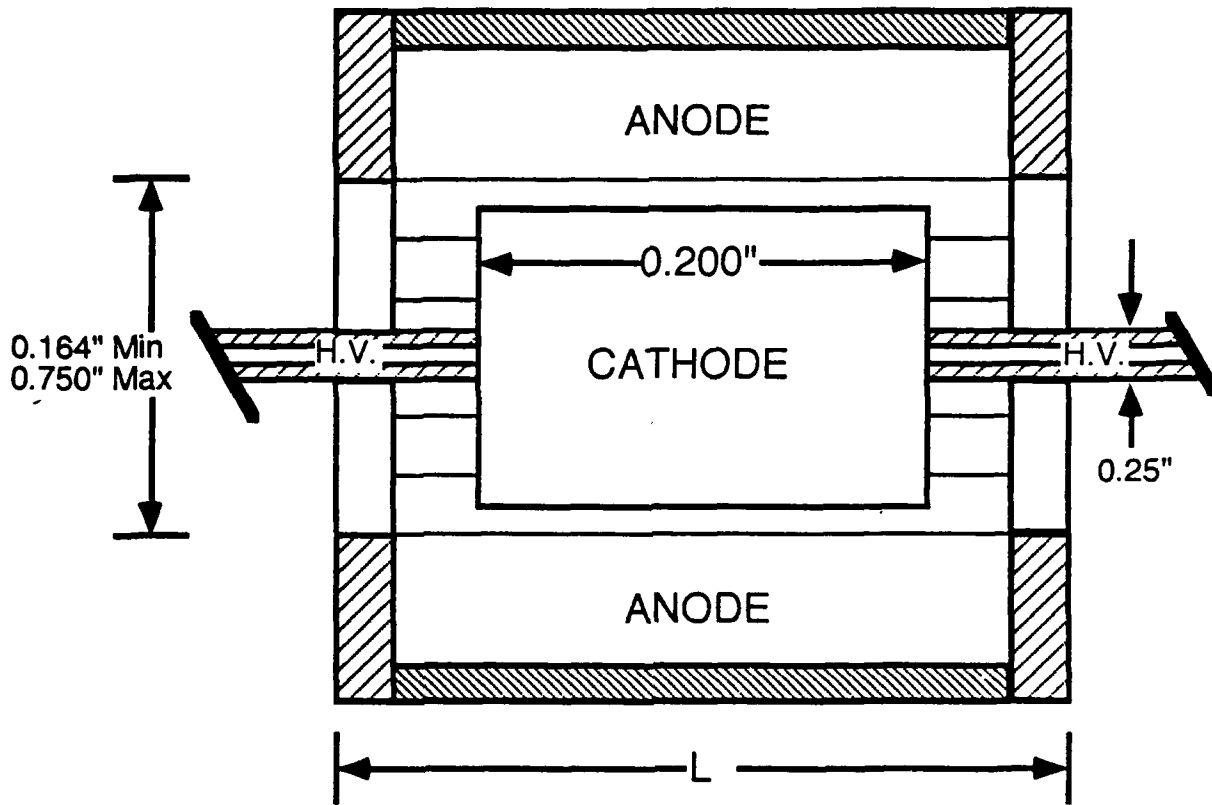


Figure 1. Longitudinal cross section of magnetron.

$$A_M B_M = 503 \text{ kMx} \quad (2)$$

where A_M is the cross-sectional area of the supply magnet and B_M is given by

$$B_M = B_R - H_W \quad (3)$$

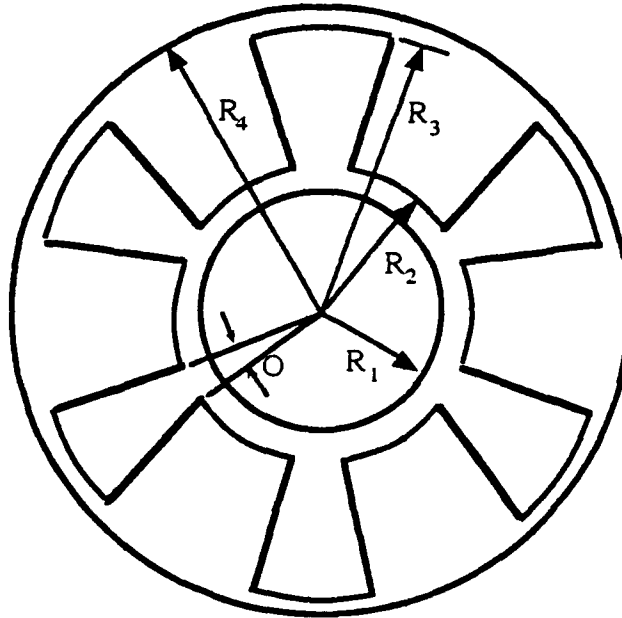
where B_R is the remanence of the magnetic material used, so

$$A_M = 112 \text{ cm}^2 \quad (4)$$

To keep the flux confined to the space within R_1 we need a tapered, radially oriented, cladding magnet encasing the longitudinal supply magnet as shown in Figure 4. The maximum thickness t_r of the former magnet is given by reference 2 as

$$t_r = H_W L_W / 2B_R = 2.25 \text{ cm} \quad (5)$$

where L_W is the length of the working space.



R ₁ Cathode O.R.	1.58 cm	0.62 inch
R ₂ Anode I.R.	2.11 cm	0.82 inch
R ₃ Anode O.R.	4.11 cm	1.62 inch
R ₄ Anode Block O.R.	4.62 cm	1.82 inch
O Cavity Angle	20 degrees	
L Circuit Length	7.20 cm	2.83 inches

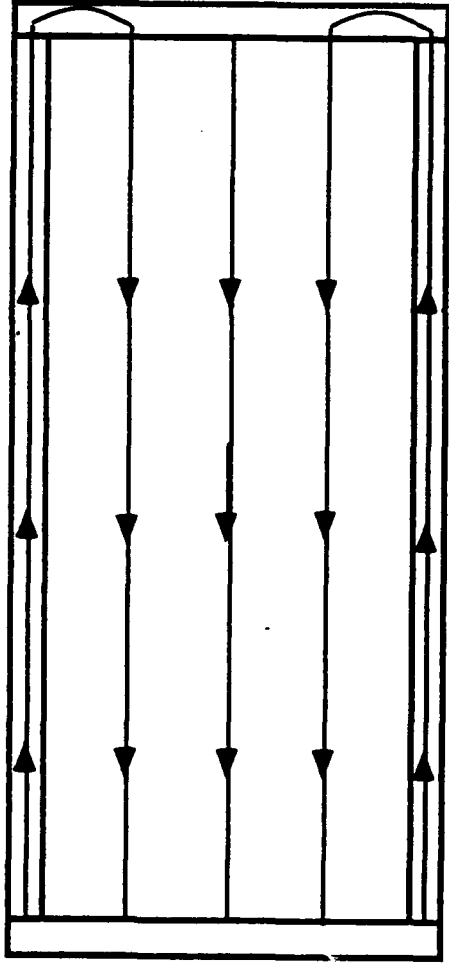
Figure 2. Transverse cross section of magnetron .

To prevent end losses, we must have disc-shaped bucking magnets, pole pieces and tapered ring-shaped corner magnets as shown in Figure 4. The bucking magnets must have a thickness equal to t_r of the radial annular magnet, namely 2.25 cm. The pole pieces must be of sufficient thickness to carry 503 kMx of flux. If iron is used with a saturation induction of 20 kG, the circumferential area A_p of each disc is given by

$$A_p = 503 \text{ kMx} / 20 \text{ kG} = 25.2 \text{ cm}^2 \quad (6)$$

so that the thickness of the pole piece must be at least

$$t_p = A_p / 2\pi R_4 = 0.866 \text{ cm} \quad (7)$$



(a)

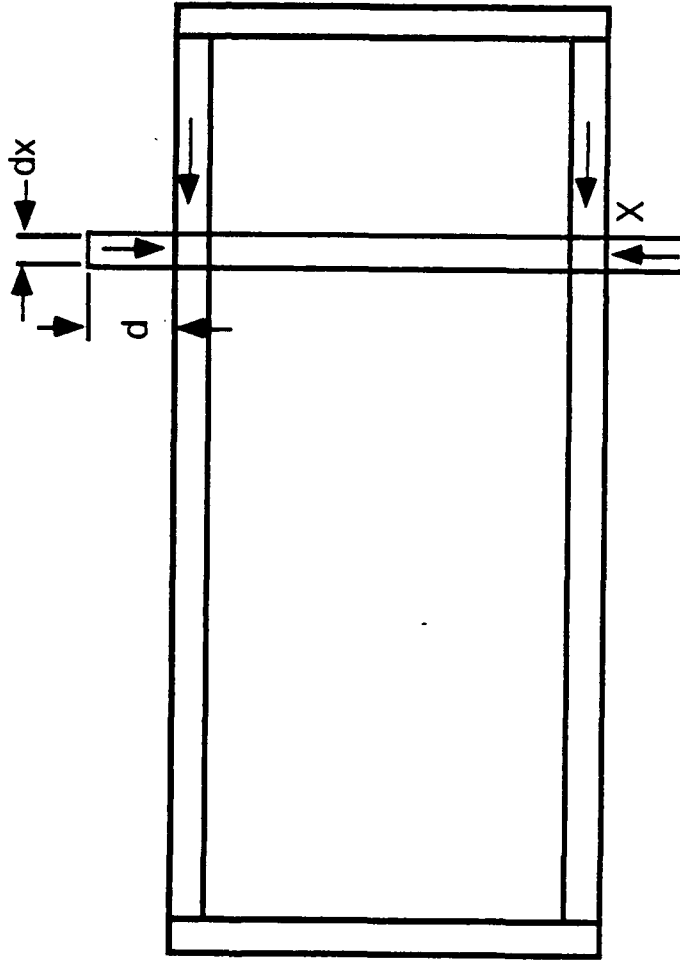
$$H_M = H_W$$

$$B_M A_M = H_W A_W$$

$$B_M = \mu H_M + B_A$$

$$A_M = A_W / (\mu_A - B_A / H_W)$$

for $H_W < 0$



(b)

$$H_C d = H_M x$$

$$d = H_W x / H_C$$

Figure 3. (a) Determination of supply magnet cross-section.
 (b) Determination of cladding thickness.

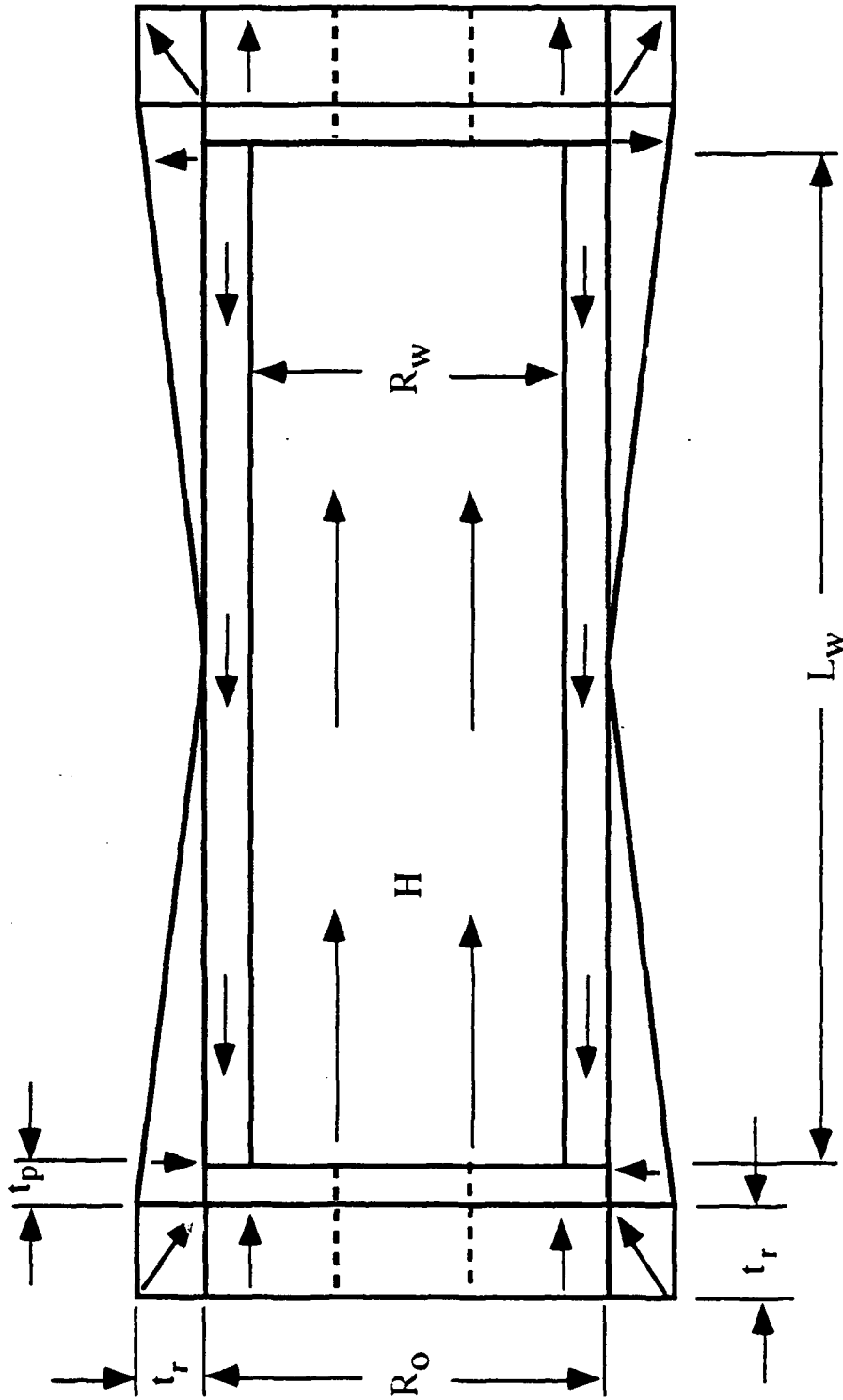


Figure 4. Design for a traditional symmetrically cladded constant field permanent magnet solenoid.

PRELIMINARY INVESTIGATION: POSSIBLE CONFIGURATIONS

Figure 5 shows the three possibilities investigated.

A. IDEAL CASE: A magnetic material of $B_R = 12$ kG is used for all magnets and all of the supply magnet, 41.9 cm^2 is placed in the interior of the tube. Part of the magnet material, 7.84 cm^2 , is placed in the central core within the cathode and the remainder, 34.1 cm^2 , is placed in the space available within the anode block. The total mass of this structure, when permanent magnets with $\rho = 7.7 \text{ g/cm}^3$ are used, is approximately 11.3 kg. A 2-D finite element plot of the structure is shown in Figure 6. As can be seen, the field uniformity over the entire region of the structure is very good. Figure 7 shows the field profile along the length of the interaction region. The field is 6.5 kOe over most of the range with a 5.6% decline towards the edges of the tube. The 7% leakage due to imperfect cladding accounts for the 6.5 kOe peak field in a configuration designed to yield a 7.0 kOe field. Entry ports for the wave guide require that part of the cladding be removed. This adds to the leakage of flux and results in further reduction in peak magnetic field.

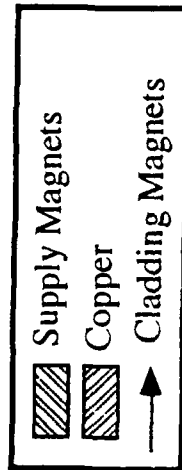
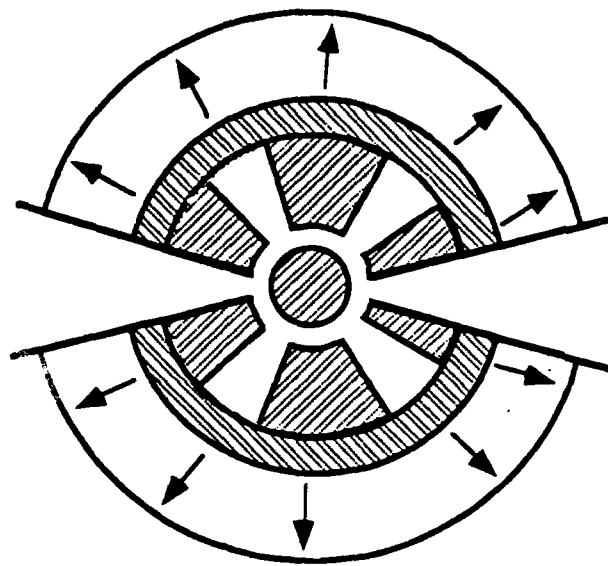
This ideal configuration yields a very compact low-mass device. However, it uses all the available space within the magnetron tube, leaving no room for cooling systems which are necessary for effective heat transfer. Without such transfer, the magnet warms up to a high temperature which results in a decrease in magnet remanence and hence magnetic field. Moreover, the commercial availability of magnetic materials of remanence 12 kG is suspect.

B. WORST CASE: Magnetic material of $B_R = 11.5$ kG is used for all magnets and all of the supply magnet is placed exterior to the tube and the model is designed for a peak field of 7.5 kOe. External placement of the magnetic material affords ready cooling. The dimensions of the structure were determined by a process similar to the one described earlier and it yields

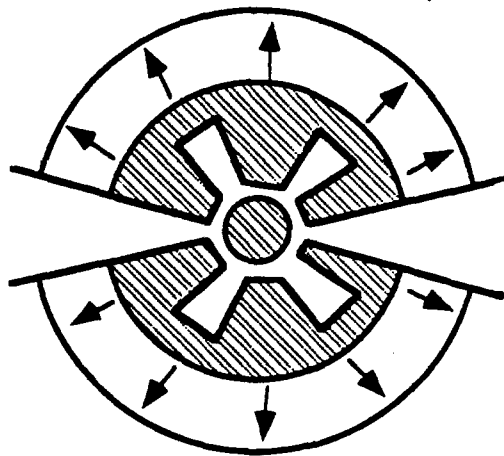
supply magnet thickness = 3.21 cm
maximum cladding thickness = 2.38 cm
thickness of pole piece = 0.511 cm
mass of magnetic structure = 23.9 kg
for magnetic materials of density $\rho = 7.7 \text{ g/cm}^3$

A 2D-finite element plot of the structure is shown in Figure 8 and the field uniformity over the entire region of the structure is remarkable. Figure 9 shows the field profile along the length of the structure. The field is 7.0 kOe for most of the circuit length with a 0.54% decline towards the edges of the tube. The leakage is about 7%.

High Temperature
 $T > 400$ K in Interior



$B_R = H_C < 12$ kG



$B_R = H_C = 12$ kG

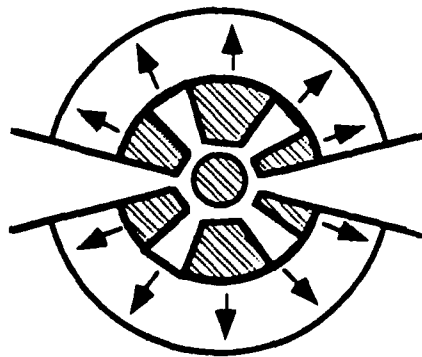


Figure 5. Three alternatives for permanent magnet placement in magnetron.

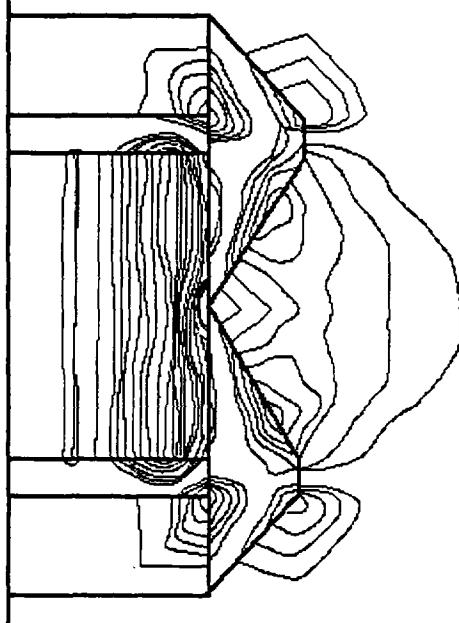


Figure 6. A 2-D finite element plot for the ideal case design.

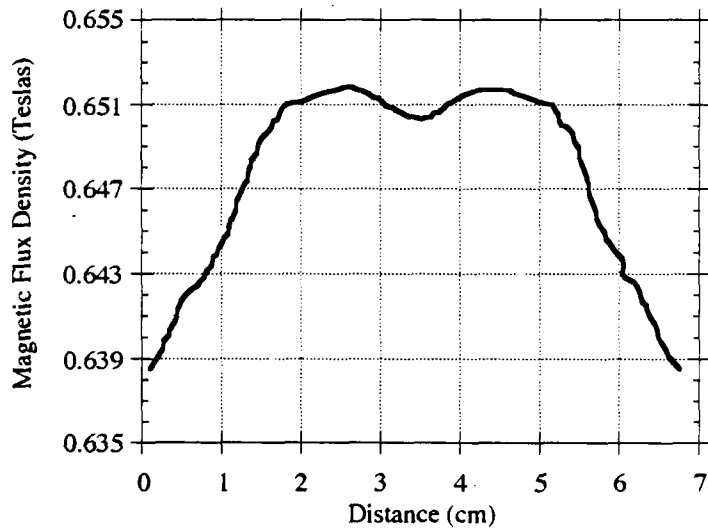


Figure 7. Field profile in the interaction region of the ideal design.

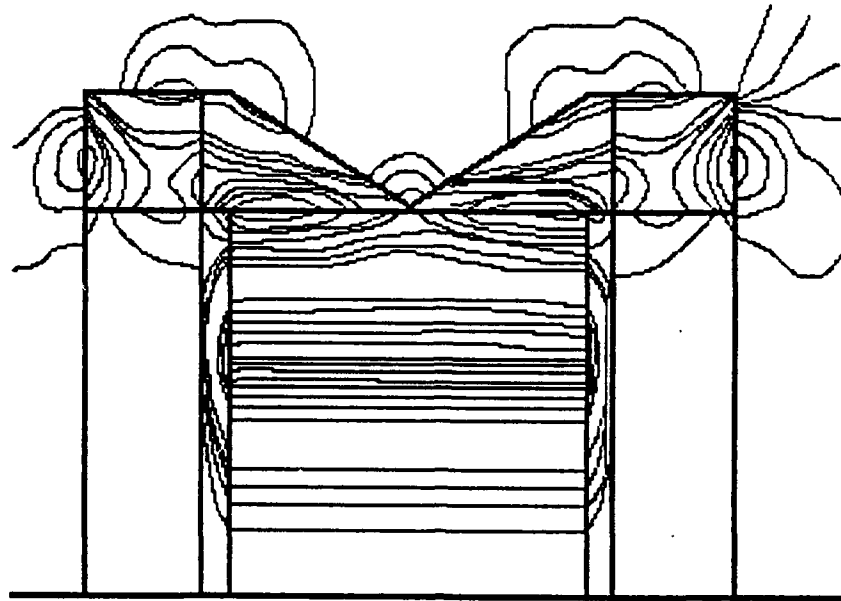


Figure 8. A 2-D finite element plot for the worst case design.

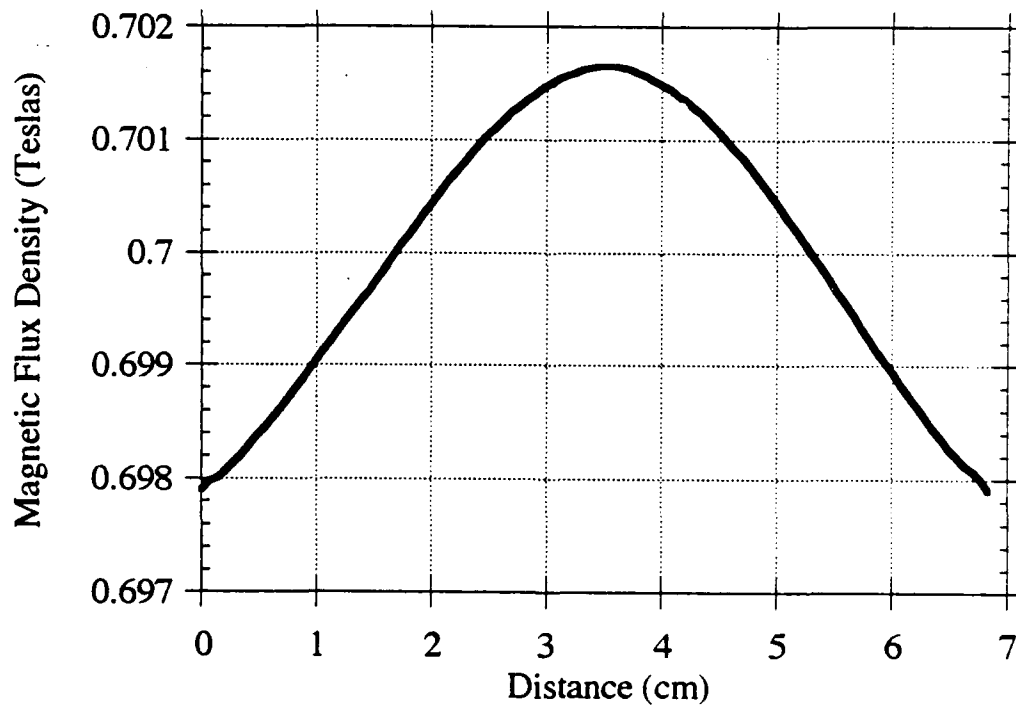


Figure 9. Field profile in the interaction region of the worst case design.

This worst case scenario yields a device that is more massive but free of complications arising from magnetic material deterioration due to heating. Adequate room exists for strategic placement of cooling systems which will ensure good magnetic field quality during operation. As in the ideal case, part of the cladding magnet has to be removed to allow for insertion of waveguides. The flux leakage at the insertion site is unavoidable. Also, this configuration demands that part of the supply magnet be removed as well. As long as the portion of the removed supply magnet is included elsewhere in the arrangement, it is rather forgiving as far as placement site is concerned. It does, however, push the cladding further out, resulting in an additional increase in mass.

C. INTERMEDIATE CASE: A theoretical assessment was also made for an intermediate arrangement, shown in Figure 10. Part of the magnetic material is placed within the magnetron tube inside the cathode, and the remainder outside the anode block. For a magnetic material of remanence $B_R = 11$ kG and $\rho = 7.7$ g/cm³, the expected mass of this configuration would be 13 kg. The smaller B_R chosen for this case reflects the probability of greater heating due to closer proximity of magnetic material to the interaction region, as the required temperature stability is available only in materials with a B_R of less than 11 kG.

The results of the three possibilities analyzed in the preliminary investigation are summarized in the table presented in Figure 11.

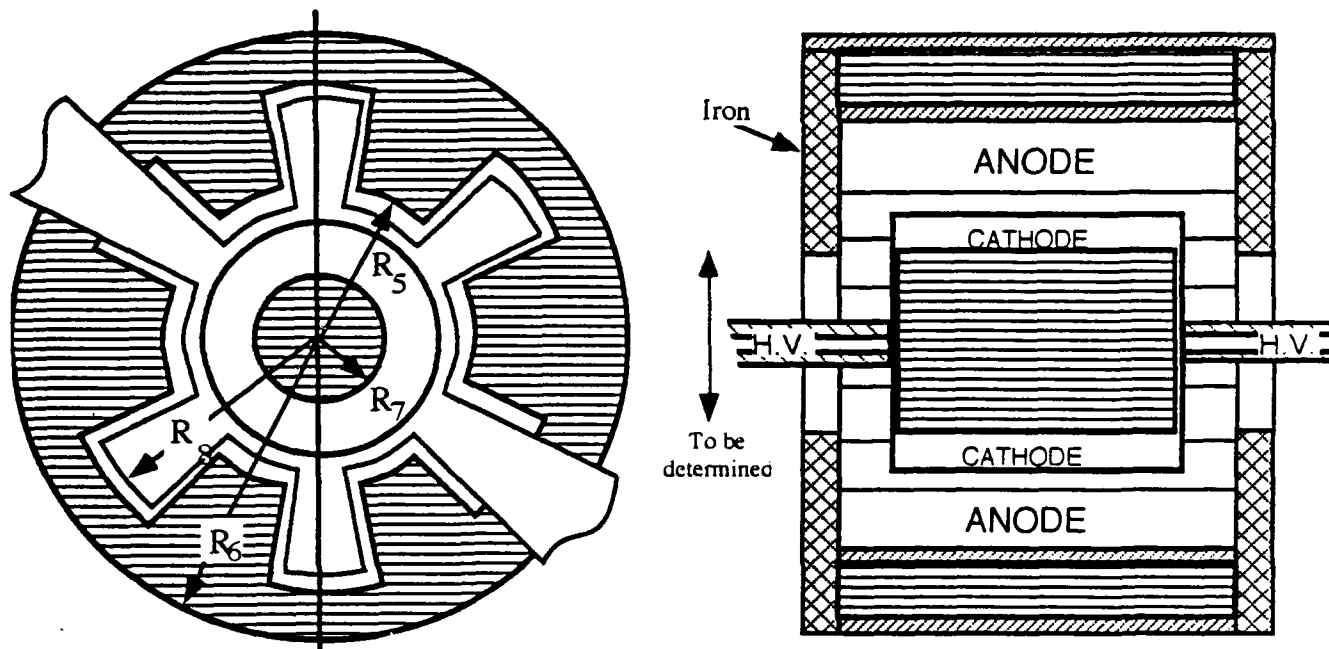
EFFECT OF WAVEGUIDE PORTS ON FIELD UNIFORMITY

An exact treatment of field irregularities resulting from missing cladding at the waveguide portals of the ideal structure was made when a computer program for three dimensional analysis became available. Originally, an estimate of the magnitude of the effect was gleaned from a computation of the field contribution H_S of the side cladding taken together with the pole pieces. The field contribution of the missing cladding H_M everywhere in the interaction region was then found to be of the order of

$$H_M \approx (40/360)H_S = H_S/9$$

The variation of H_M around the circumference of the interaction region ΔH_M is very much smaller than H_M itself so that

$$\Delta H_M \ll H_M = H_S/9$$



DIMENSIONS

R_5 - Magnetic Material Inner Radius	2.60 cm (1.02 in)
R_6 - Magnetic Material Outer Radius	To be determined
R_7 - Cathode Region Magnet Outer Radius	1.27 cm (0.5 in)
R_8 - 2nd Magnetic Material Inner Radius	4.11 cm (1.62 in)

* Note: R_5 and 0.100 Dim allow for possible cooling channels

Figure 10. Magnet location in the intermediate choice.

and since H_S is only one percent of the total field, the effect of H_M is expected to be negligible. The three-dimensional analysis confirmed this conclusion as it showed an azimuthal field variation of only a few parts per thousand as is shown in the plot of Figure 13. More details of the analysis are given in the appendix.

No.	Scenario	Description	Mass	Leakage	Variation
1	Ideal Case	Magnet of Remanence = 12 kG All in the tube interior	11.5 kg	7%	6900 - 7000 G
2	Worst Case	Magnet of Remanence = 11.5 kG All exterior to tube	23.85 kg	7%	6980 - 7000 G
3	Intermediate Case	Magnet of Remanence = 11 kG Partially exterior to tube			

Figure 11. Magnet mass and magnetic field summary for the three choices.

FINAL ANALYSIS

In the final analysis, it was determined that in view of the quality of commercially available magnetic materials and the need to effectively remove the heat generated within the tube, all the magnet material be placed in a traditional configuration outside the anode block. Easily available permanent magnet materials of remanences $BR = 10 \text{ kG}$ and density $= 7.7 \text{ g/cm}^3$ were used in the analysis. A structure was designed for a theoretical 7.0 kOe field in the interaction region. The mass of this configuration was considerably higher, 25.7 kg . The 2-D finite element plot of Figure 12 shows the field uniformity to be very good in the interaction region. Figure 13 shows that the field along the length of that region is about 6.0 kOe and is uniform to about 0.29% , indicating a flux leakage of approximately 7% , again because of imperfect cladding.

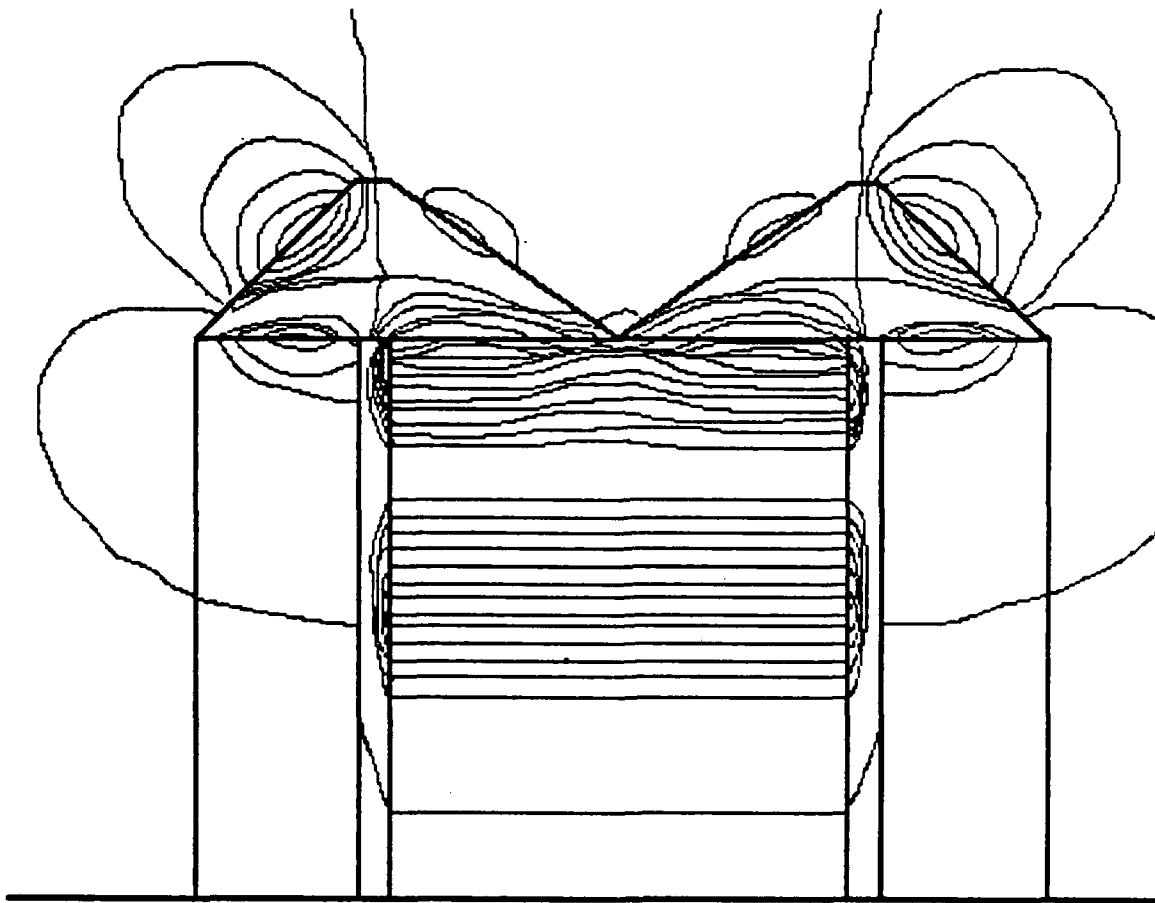


Figure 12. A 2-D finite element plot for the most practical design. Here the usual corner magnets of rectangular cross-section have been replaced by the equally effective and simpler radially oriented magnets of triangular cross-section.

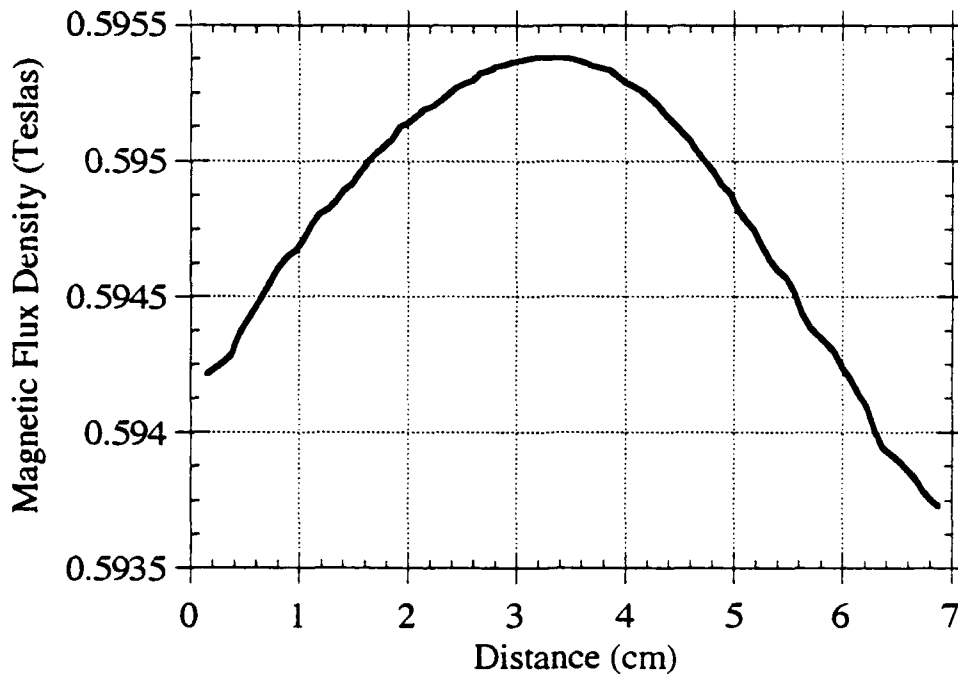


Figure 13. Field profile in the interaction region of the best choice.

Further modifications were then introduced as dictated by the electronics of the tube. To serve as possible entry and exit ports for electronic and thermal gadgetry, tunnels of varying diameter drilled at both ends of the above permanent magnet device were considered in the analysis. Figure 14 tabulates the peak fields and the field gradient along the length of the interaction region for a variety of models considered. Figure 15 shows the variation in peak field as a function of tunnel radius, a major factor in evaluating the possibilities before a judgment can be made with regard to a choice in hole diameter.

The possibility of increasing the tube length to 9.2 cm was also investigated. Although this would further add to the mass of the device, it would ensure field uniformity over the entire region of the rf output where the waveguides are inserted. The results are included in Figures 14 and 15.

CONCLUSIONS

A prototype of the 7.2 cm long permanent magnet described above is under consideration. Magnetic materials such as $\text{Sm}_2\text{Co}_{17}$ ($\rho = 8.3 \text{ g/cm}^3$) and Nd-Fe-B ($\rho = 7.4 \text{ g/cm}^3$) are possible choices. The remanences of commercially available materials and their sensitivities to high temperatures would determine the final choice. The 7.0% leakage encountered throughout the investigation can be eliminated easily by a slight modification of the cladding as described in references 1 and 2.

No.	Filename and Mass kg	Desired Field kOe	Magnet remanence kG	Bore Radius cm	On-axis Field (G)		On-axis Field (G) delta	Air gap Field (G)		Air gap Field (G) delta	Field across Work Space Oe
					max	min		max	min		
1	MM4 25.75	7	10	0	5952	5937	.25%	5954	5937	.29%	5962-5952
2	MM8 25.75	7	10	.3475	5928			5952	5940	.20%	5961-5948
3	MM12 25.25	7	10	.4166	5923			5950	5942	.13%	5961-5945
4	MM9 25.75	7	10	.5	5916			5947	5940	.12%	5960-5940
5	MM10 25.75	7	10	1	5831			5906	5888	.31%	5950-5864
6	MM13 25.25	7	10	1.5	5650			5788	5750	.66%	5933-5686
7	MM11 25.25	7	10	1.905	5418			5670	5490	3.3%	5910-5447
8	MMX1 37.96	7	10	0	5900	5873	.46%	5904	5870	.6%	5927-5900
9	MMX2 37.96	7	10	-.4166	5878			5900	5874	.46%	5924-5895
10	MMX3 37.96	7	10	1	5823			5866	5838	.45%	5910-5851
11	MMX4 37.96	7	10	1.905	5572			5737	5456	5.2%	5853-5602

Figure 14. Permanent magnet choices for magnetrons: A summary.

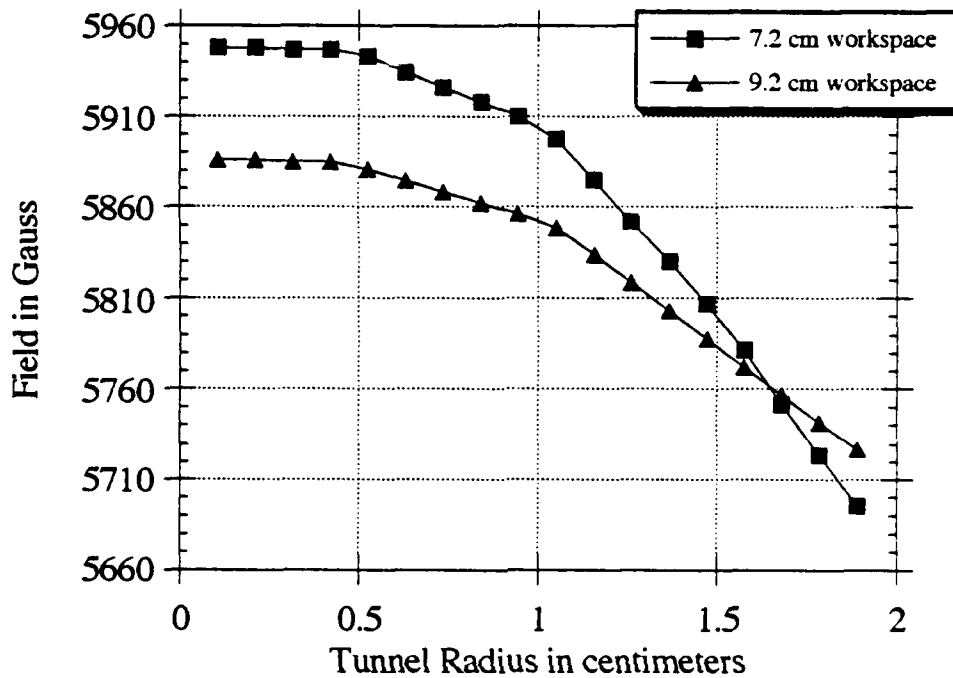


Figure 15. Peak field at electron orbit site as a function of the tunnel radius.

REFERENCES

1. H. A. Leupold, E. Potenziani II, D. J. Basarab and A. S. Tilak, "Magnetic field source for bichambered electron-beam devices"; J. Appl. Phys. **67**(9), (1990)
2. E. Potenziani II and H. A. Leupold, IEEE Trans. Magn., **MAG-22**(5), 1078(1986)
3. J. P. Clark and H. A. Leupold, IEEE Trans. Magn., **MAG-22**(5), 1063(1986)

APPENDIX A • Three-Dimensional Analysis

A three dimensional finite element analysis (FEM) was performed on the structure illustrated in Figure A-1. Figures A-2 thru A-5 show several cross-sectional cuts through the structure perpendicular to the axis of rotation. The various magnet orientations are shown by heavy arrows and all magnets were assumed to have a remanence of 10 kG (795,774 amps/meter).

Because computer disk and RAM requirements quickly grow to unmanageable proportions as problem complexity increases, we have used symmetry arguments to greatly simplify this analysis. Only one-half the length of the structure in the z-direction is modeled and this end "surface" is left unconstrained. Also, only 180° of the structure in the azimuthal direction is modeled. The resulting flat "surface" in this case is constrained to $A_x=A_z=0$ (where \vec{A} is the vector potential). The slot for the waveguide extends from 80° to 100° in the azimuthal direction (by symmetry, there exists an identical waveguide slot in the opposite half of the structure that extends from 260° to 280°). A center hole size of 0.5 cm diameter was chosen for this analysis.

Figure A-6 is an overall view of the structure and Figure A-7 is the resulting FEM mesh. The structure is tilted down 25° about the x-axis and bulges outwards towards the reader.

The z-component of the magnetic field was plotted for several different paths, as shown in Figures A-8 thru A-10. In Figure A-8, H_z is plotted, as one travels along the central axis of the structure, for several different radii. The point $z=0$ corresponds to the lowest point in the "air" working space, i.e., adjacent to the pole piece. For $r=2$ cm from the central axis, the field is relatively uniform along the length of the structure (the z-distance of 3.5 cm corresponds approximately to the midpoint of the structure along its length). For $r=0.35$ cm, the influence of the central hole (of radius 0.25 cm) is pronounced only a centimeter or less from the pole pieces.

Figures A-9 and A-10 are plots of H_z along 180° arcs of $r=2.1$ cm and $r=4.5$ cm from the central axis. The horizontal axis corresponds to distance **along** each arc. The influence of the waveguide slit (at 80° to 100°) can be seen as a small decrease in field component in the middle third of each arc.

Overall, the variation in field in the entire working space is on the order of a few percent, but if one keeps to a particular path with a high degree of symmetry (e.g., an electron beam in a circular orbit around the central axis), a variation on the order of a few tenths of a percent can be realized. A detailed printout of all fields and related parameters is included.

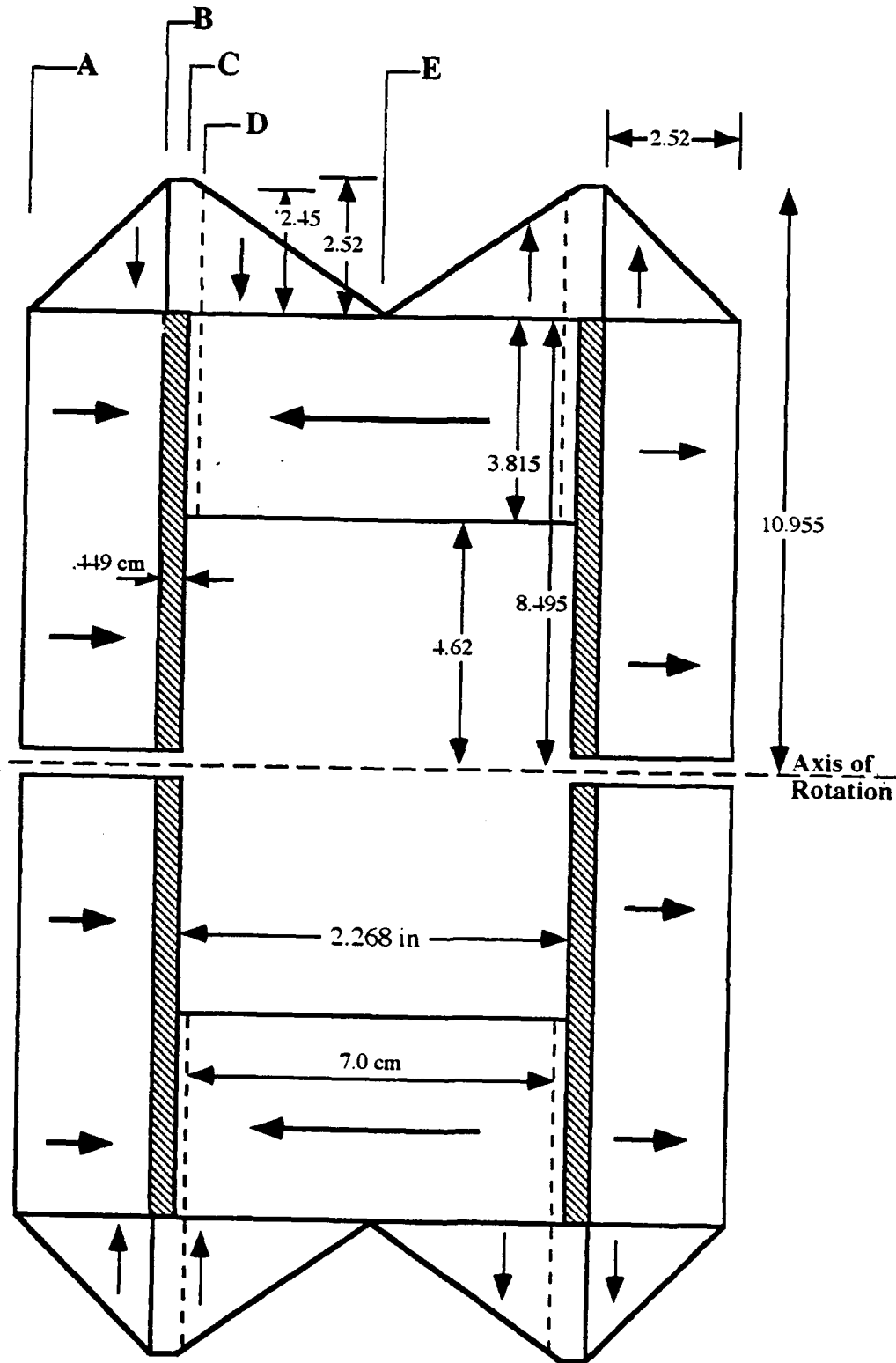


Figure A-1. Side view of the overall structure as used in the three-dimensional analysis. Overall length is 13.126 cm.

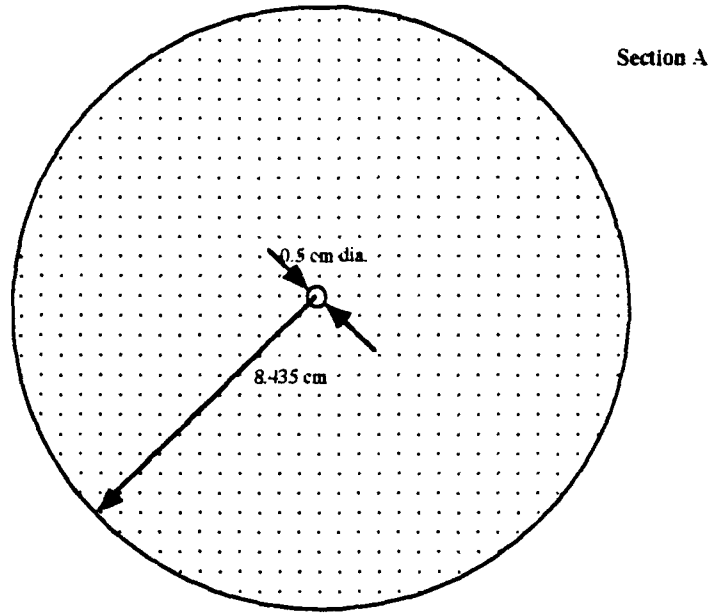


Figure A-2. View of cut through section A of figure A-1.

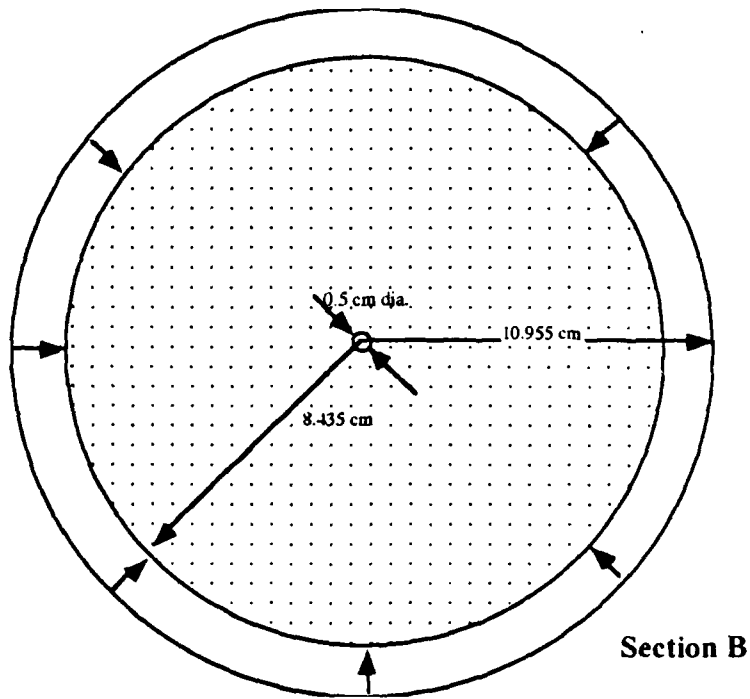
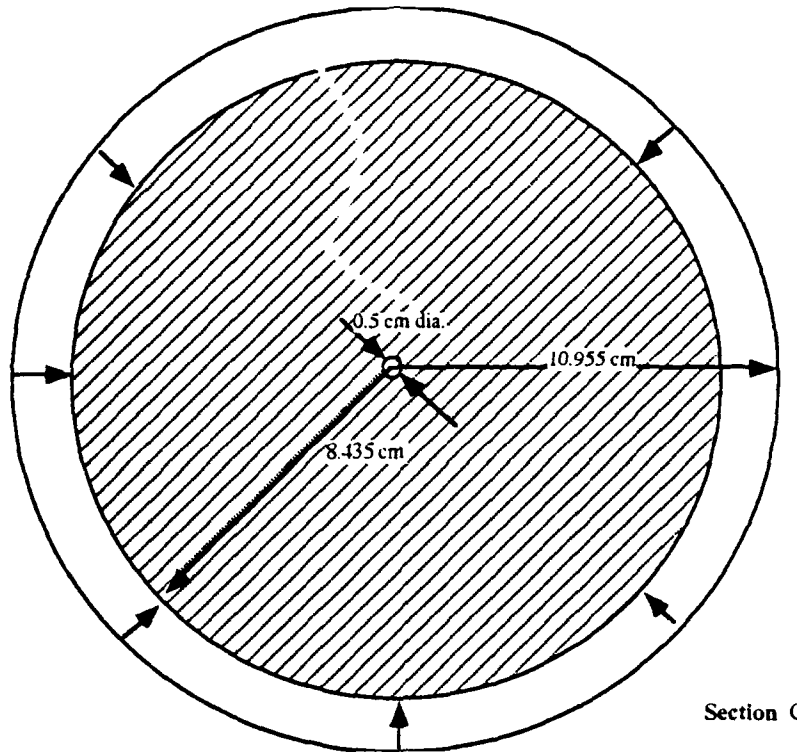
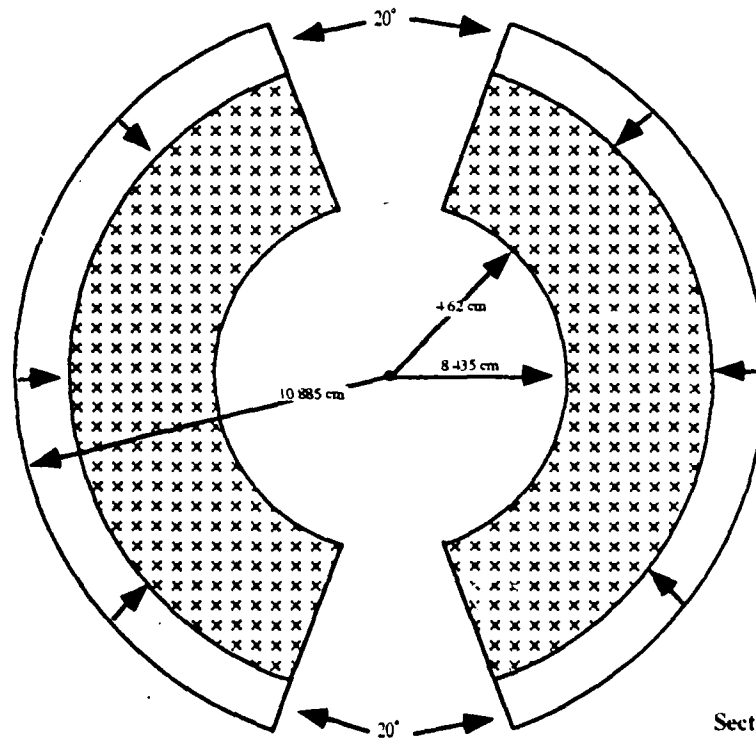


Figure A-3. Diagram of a cut through section B of figure A-1.



Section C

Figure A-4. Diagram of a cut through section C of figure A-1.



Section D

Figure A-5. Diagram of cut through section D of figure A-1.

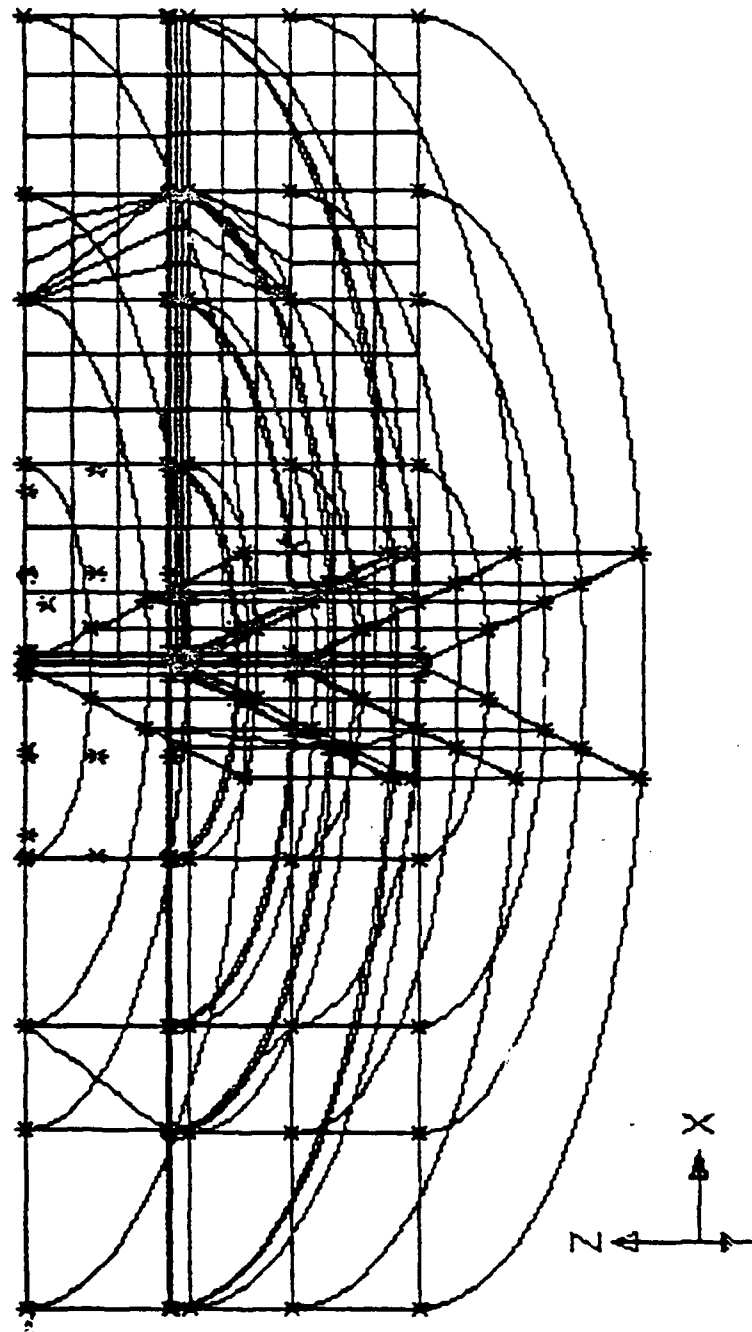


Figure A-6. Overall view of the structure modeled with one half the length and 180° around the circumference.

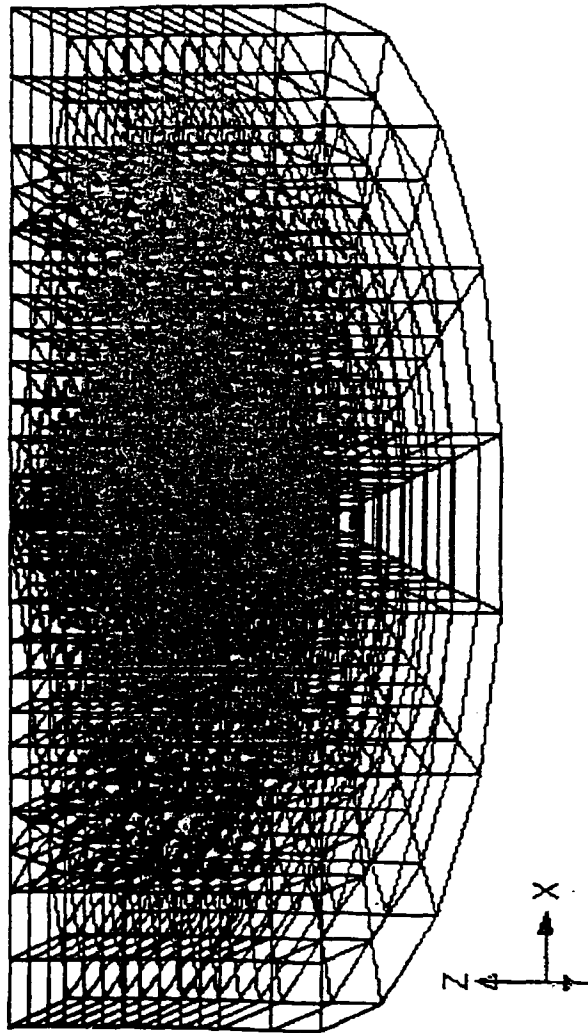


Figure A-7. Resulting three-dimensional finite element mesh of the structure as shown in Figure A-6. The structure is tilted 25° about the x-axis to make it easier to visualize.

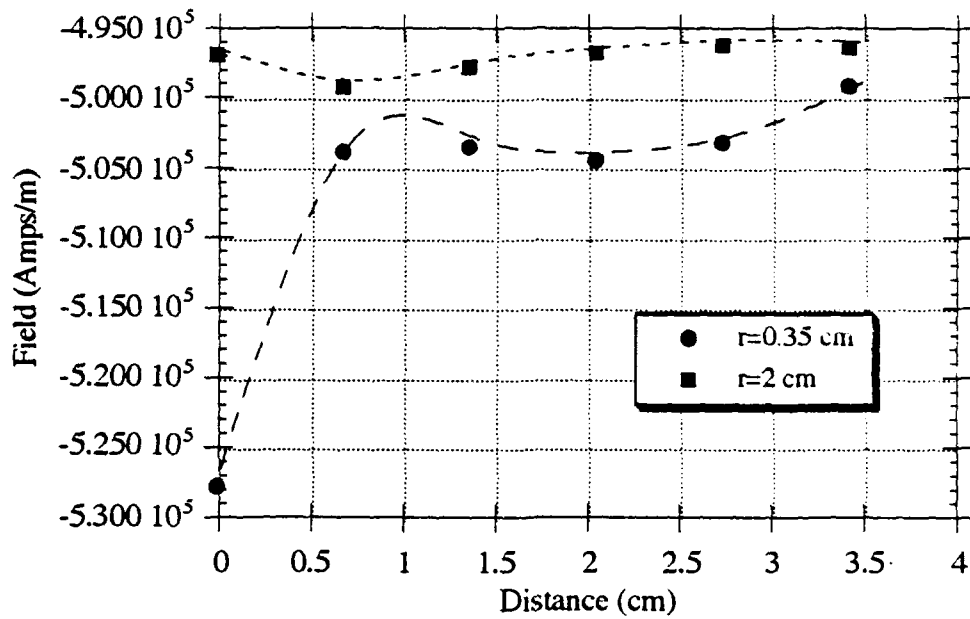


Figure A-8. H_z versus distance along z axis, $\theta=45^\circ$.

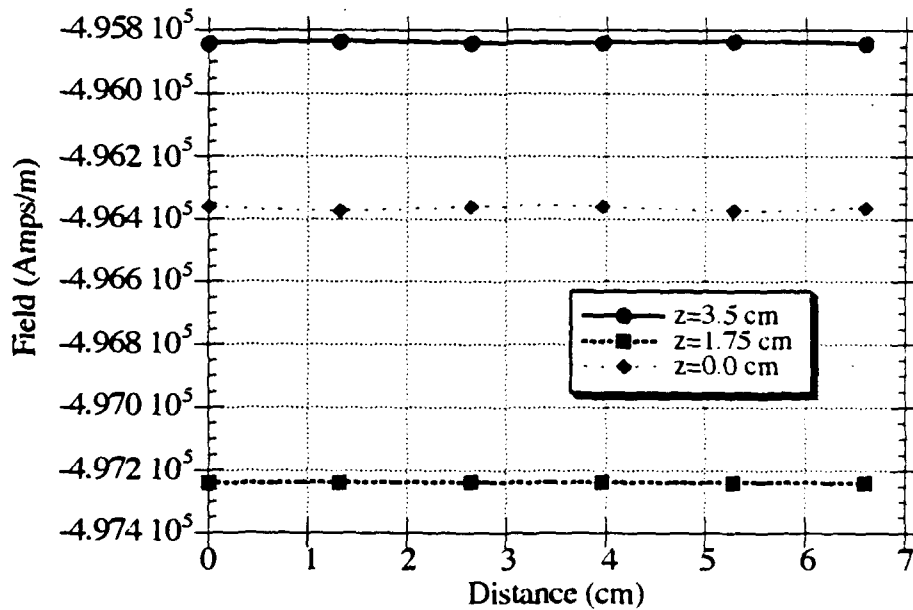


Figure A-9. H_z versus distance along arc from $\theta=0^\circ$ to $\theta=180^\circ$ at r=2.1 cm.

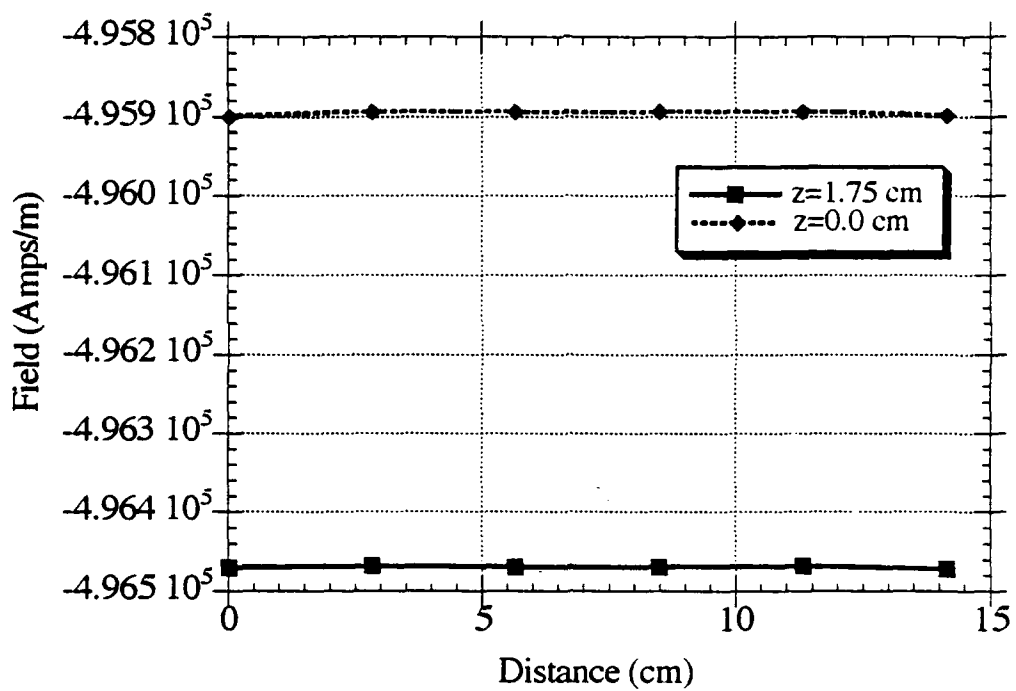


Figure A-10. H_z versus distance along arc from $\theta = 0^\circ$ to $\theta = 180^\circ$ at $r = 4.5$ cm.

ELECTRONICS TECHNOLOGY AND DEVICES LABORATORY
MANDATORY DISTRIBUTION LIST
CONTRACT OR IN-HOUSE TECHNICAL REPORTS

8 Jul 91
Page 1 of 2

Defense Technical Information Center*

ATTN: DTIC-FDAC

Cameron Station (Bldg 5)
Alexandria, VA 22304-6145

(*Note: Two copies for DTIC will
be sent from STINFO Office.)

Director

US Army Material Systems Analysis Actv

ATTN: DRXSY-MP

001 Aberdeen Proving Ground, MD 21005

Commander, AMC

ATTN: AMCDE-SC

001 5001 Eisenhower Ave.
Alexandria, VA 22333-0001

Commander, LABCOM

ATTN: AMSLC-CG, CD, CS (In turn)

001 2800 Powder Mill Road
Adelphi, Md 20783-1145

Commander, LABCOM

ATTN: AMSLC-CT

001 2800 Powder Mill Road
Adelphi, MD 20783-1145

Commander,

US Army Laboratory Command

Fort Monmouth, NJ 07703-5601

1 - SLCET-DD

2 - SLCET-DT (M. Howard)

1 - SLCET-DR-B

35 - Originating Office

Commander, CECOM

R&D Technical Library

Fort Monmouth, NJ 07703-5703

1 - ASQNC-ELC-IS-L-R (Tech Library)

3 - ASQNC-ELC-IS-L-R (STINFO)

Advisory Group on Electron Devices

ATTN: Documents

002 2011 Crystal Drive, Suite 307
Arlington, VA 22202

ELECTRONICS TECHNOLOGY AND DEVICES LABORATORY
SUPPLEMENTAL CONTRACT DISTRIBUTION LIST
(ELECTIVE)

8 Jul 91
Page 2 of 2

001	Director Naval Research Laboratory ATTN: CODE 2627 Washington, DC 20375-5000	001	Cdr, Atmospheric Sciences Lab LABCOM ATTN: SLCAS-SY-S White Sands Missile Range, NM 88002
001	Cdr, PM JTFUSION ATTN: JTF 1500 Planning Research Drive McLean, VA 22102	001	Cdr, Harry Diamond Laboratories ATTN: SLCHD-CO, TD (In turn) 2800 Powder Mill Road Adelphi, MD 20783-1145
001	Rome Air Development Center ATTN: Documents Library (TILD) Griffiss AFB, NY 13441		
001	Deputy for Science & Technology Office, Asst Sec Army (R&D) Washington, DC 20310		
001	HQDA (DAMA-ARZ-D/Dr. F.D. Verderame) Washington, DC 20310		
001	Dir, Electronic Warfare/Reconnaissance Surveillance and Target Acquisition Ctr ATTN: AMSEL-EW-D Fort Monmouth, NJ 07703-5206		
001	Dir, Reconnaissance Surveillance and Target Acquisition Systems Directorate ATTN: AMSEL-EW-DR Fort Monmouth, NJ 07703-5206		
001	Cdr, Marine Corps Liaison Office ATTN: AMSEL-LN-MC Fort Monmouth, NJ 07703-5033		
001	Dir, US Army Signals Warfare Ctr ATTN: AMSEL-SW-OS Vint Hill Farms Station Warrenton, VA 22186-5100		
001	Dir, Night Vision & Electro-Optics Ctr CECOM ATTN: AMSEL-NV-D Fort Belvoir, VA 22060-5677		